A Limb Tracking Platform for Tele-Rehabilitation

PASQUALE BUONOCUNTO, ANDREA GIANTOMASSI, MAURO MARINONI, DAVIDE CALVARESI, and GIORGIO BUTTAZZO, Scuola Superiore Sant'Anna

The adoption of motor-rehabilitative therapies is highly demanded in a society where the average age of the population is constantly increasing. A recent trend to contain costs while providing high quality of healthcare services is to foster the adoption of self-care procedures, performed primarily in patients' environments rather than in hospitals or healthcare structures, especially in the case of intensive and chronic patients' rehabilitation.

This work presents a platform to enhance limb functional recovery through telerehabilitation sessions. It relies on a sensing system based on inertial sensors and data fusion algorithms, a module to provide bio-feedback tailored to the users, and a module dedicated to the physicians' practices. The system design had to face several cyber-physical challenges due to the tight interaction between patient and sensors. For instance, integrating the body kinematics into the sensory processing improved the precision of measurements, simplified the calibration procedure, and made it possible to generate bio-feedback signals. The precision of the proposed system is presented through a set of experiments, showing a resolution below one degree in monitoring joint angles. A validation of the proposed solution has been performed through a medical trial on 50 patients affected by osteo-articular diseases.

The presented framework has been designed to operate in other application fields, such as neurological rehabilitation (e.g., Parkinson, Stroke, etc.), sports training, and fitness activities.

CCS Concepts: • **Networks** → **Cyber-physical networks**; *Sensor networks*; • **Applied computing** → **Health care information systems**; • **Computer systems organization** → **Embedded and cyber-physical systems**; Embedded hardware; Embedded software; Real-time system architecture; • **Hardware** → *Wireless integrated network sensors*;

Additional Key Words and Phrases: Telerehabilitation, limb tracking, inertial sensors, wireless sensor networks

ACM Reference format:
Pasquale Buonocunto, Andrea Giantomassi, Mauro Marinoni, Davide Calvaresi, and Giorgio Buttazzo. 2018. A Limb Tracking Platform for Tele-Rehabilitation. *ACM Trans. Cyber-Phys. Syst.* 2, 4, Article 30 (September 2018), 23 pages.
https://doi.org/10.1145/3148225

1 INTRODUCTION

By 2050, the growing number of elderly people will have a significant impact on social assistance and health care institutions (Iarlori et al. 2014; Calvaresi et al. 2017). Medical advances enable the population to live longer in good health than in the past, but much more is still needed for

This work has been partially supported by Telecom Italia.
Authors' addresses: P. Buonocunto, A. Giantomassi, M. Marinoni, D. Calvaresi, and G. Buttazzo; emails: {p.buonocunto, a.giantomassi, m.marinoni, d.calvaresi, g.buttazzo}@sssup.it.

https://doi.org/10.1145/3148225

disease prevention and home care (Calvaresi et al. 2014). One of the main factors that progressively reduces the mobility of elderly people is the onset of osteo-articular diseases of the skeletal system. Currently, these problems are treated by drugs as far as possible; however, surgery is emerging with innovative and more effective techniques that are less and less invasive.

Nevertheless, the postoperative rehabilitation is often very long and the occurrence of complications is quite common, even several weeks or months after the surgery, leading to a significant increase in public health cost, or to a reduced quality of service because of lack of adequate resources.

To cope with such growing needs, it would be desirable to manage the rehabilitation in a more efficient and effective way, by reducing the access time to the structures by patients and allowing the personnel to follow a greater number of patients maintaining or even increasing the quality of service (Cesarini et al. 2015). Telemonitoring enables the possibility of transmitting some interesting parameters to a remote location for the clinical evaluation of patients who require continuous monitoring of their health conditions (Hailey et al. 2011).

Tele-rehabilitation is one of the special fields of telemedicine's application and indicates the remote use of rehabilitation services using telecommunications technology as the service delivery medium (Russel 2007), thereby minimizing the barriers of distance, time, and cost. More specifically, telerehabilitation can be defined as "the application of telecommunication, remote sensing, operation technologies, and computing technologies to assist with the provision of medical rehabilitation services at a distance" (Cooper et al. 2001). The diffusion of telerehabilitation systems would lead to a number of advantages, both for the patient and the hospital structure (Benettazzo et al. 2014; Calvaresi et al. 2015), in terms of cost, time, and services.

To achieve these advantages, the objective of a telerehabilitation program is to develop and validate advanced ICT systems and clinical protocols for delivering remote rehabilitation treatments (i.e., home-based rehabilitation programs), thus improving both the objective and subjective results of patients, increasing accessibility to rehabilitation services, and creating the least restrictive environment.

Another fundamental aspect regards patients' adherence and acceptability, which may be limited by motor (e.g., endurance), non-motor (e.g., fatigue, pain, dysautonomic symptoms) motivational, and cognitive deficits. To overcome these pitfalls, a program of exercising has to be easy to reach daily, exciting and has to promote motivation and adherence. Moreover, it is remarkable that, to be effective, rehabilitation has to be meaningful, task-oriented, intensive, and context interactive (e.g., through virtual reality). Moreover, the exercise has to be quantifiable and monitored in real time to provide useful feedback to the patient (Giantomassi et al. 2014). For patients affected by multiple disabilities, a multi-modal feedback (e.g., visual, haptic, and auditive) may be necessary to still be effective (Cesarini et al. 2016).

Another crucial challenge that must be addressed to fruitfully apply telerehabilitation is related to the wearing phase necessary to position the sensors on the limbs to be monitored. In fact, if the patient is not supported in the dressing phase, errors in the sensors placement can jeopardize the final measures. Such a phase posed serious limitations for an effective adoption of telerehabilitation solutions.

Satisfying all the requirements defined for users, clinical personnel, and security needs entails different challenges in the development of a telerehabilitation framework.

Contributions

This article makes the following novel contributions:

— It proposes a telerehabilitation framework with a high degree of customization for supporting therapists and patients from the pre-surgical condition to the rehabilitation phases. The

adoption of such a framework allows identifying and monitoring the patient's conditions during all the surgical and rehabilitation phases. The framework also allows the physician/therapist to define the set of exercises needed for the therapy program and configure the system to provide the proper feedback according to the specific exercises and patient needs. The presented framework is an extension of the one proposed in Cesarini et al. (2014).

—It presents an innovative low-cost wearable device with sufficient accuracy, easy connectivity, and long battery lifetime, overcoming the major limitations of existing sensors on the market that hinder or limit the spread of telerehabilitation. The sensor illustrated in this article represents the second generation of the one described in Buonocunto and Marinoni (2014).

—It describes ReHapp, an Android application for integrating the data produced by the sensors and present them to the patient and the physician through distinct graphical user interfaces.

—It presents a self-calibration algorithm to support the user in the wearing phase and compensates positioning errors by an adaptive algorithm that takes into account the body kinematics to detect the actual sensors placement. Once the anatomical joints are identified, the rehabilitation program can start, and the algorithm provides anatomical angles of interest for the specific exercise.

Paper structure

The rest of the article is organized as follows. Section 2 illustrates the framework architecture and its main components. Section 3 presents the sensors developed within the context of the proposed framework. Section 4 presents the devised technique to detect the actual sensors placement and the data fusion algorithm to measure the rehabilitation performance. Section 5 presents the user interface designed to provide the feedback to the patient. Section 6 reports some experimental results carried out on the system to characterize its behavior. Finally, Section 7 states our conclusions and future work.

2 TELEREHABILITATION FRAMEWORK

The integration of sensing devices within a more comprehensive framework is crucial to exploit all their capabilities and enable their use in a real clinical environment.

The proposed system is characterized by the seamless integration of physical components and their cyber models with computation and communication elements. It is thus classifiable as a proper cyber-physical system (CPS) (Calvaresi et al. 2017a), integrating a distributed sensing system (wearable sensors) and a computing platform (tablet and cloud-based services), designed taking into account physical characteristics (body-kinematics models and constraints) and human-machine interactions (with physicians and patients) (Rajkumar et al. 2010). This section describes the main components of a telerehabilitation framework to support the patient and the therapist during lower limbs functional recovery. This framework aids patients in the execution of rehabilitation exercises by monitoring the limb movements using a set of wearable nodes and providing them with multi-modal bio-feedback (e.g., visual, haptic, and auditive) to improve the quality of the performed activities. The system is also designed to assist the therapist during the definition of the exercises, which can be tailored to the patient. The information collected during the session is uploaded to a cloud infrastructure for storage and further analysis. The result of the analysis can then be accessed by the therapist to follow the patient's progress and possibly tune the therapy.

The proposed telerehabilitation framework is illustrated in Figure 1 and consists of three main components, described in detail in the rest of this section: a *patient support module*, a *physician support module*, and a set of *cloud based services*.

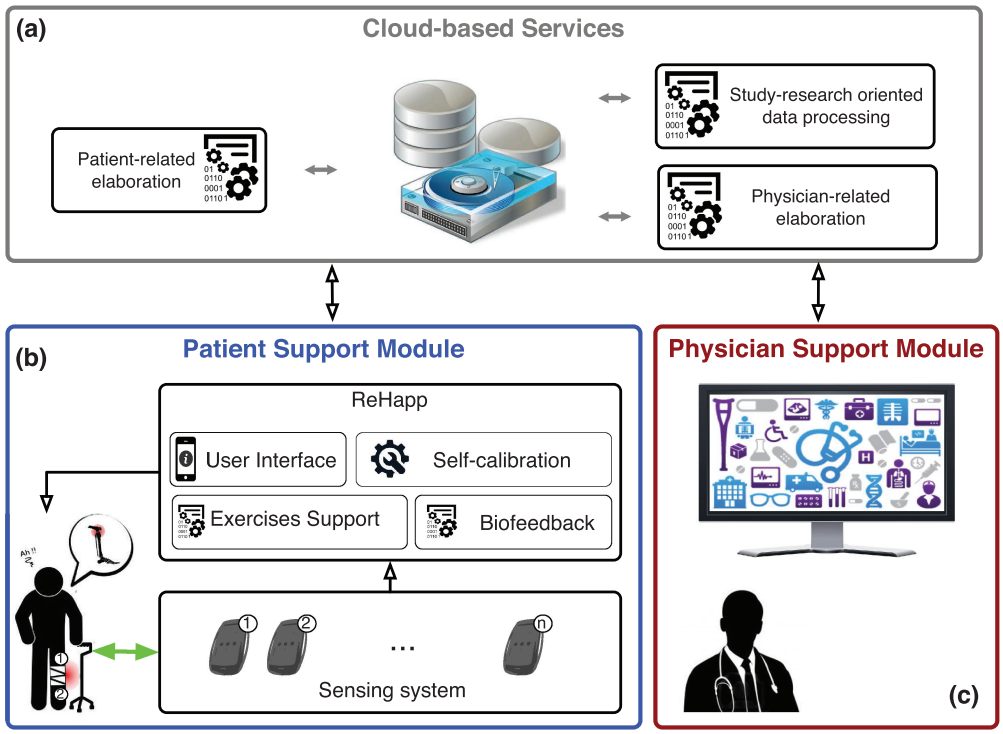

Fig. 1. The proposed telerehabilitation framework: (a) Patient Support Module, (b) Cloud-based Services, and (c) Physician Support Module.

2.1 Patient Support Module

The main purpose of this module is to aid the patient in wearing the sensors and support him/her during the execution of the rehabilitation exercises. It consists of a set of wearable sensing nodes, a bio-feedback generation unit, and a data processing software running on a mobile device. Note that, in the specific case study of knee rehabilitation considered in this article, the system makes use of two wearable sensing nodes, placed as shown in Figures 1(b) and 6.

Sensing Module. The main concept behind the sensing subsystem is the acquisition of the information needed to evaluate the exercise without changing how the patient executes it. To obtain such a result, the sensor has to be small, lightweight, and comfortable to wear. Moreover, the setup procedure performed before the session must be simple and assisted by a software guiding the patient during sensors placement. This is a crucial step to obtain meaningful and accurate data for the analysis.

Exercise Performance Evaluation. This software module analyzes the sequence of data recorded during the execution of the exercise, evaluating its performance with respect to a reference trajectory executed with the supervision of the therapist. The analysis produces a number of performance indices that will later be assessed by the physician to establish the progress of the patient and possibly updates the therapy.

Bio-Feedback. The bio-feedback is a very important aspect to be considered during the execution of an exercise, because it provides information back to the patient to promptly correct possible

erroneous movements. Thus, guiding the patient towards the execution of the intended motion, while correcting him/her through a mix of stimuli is of paramount importance. Different types of feedback can be conveniently conveyed by the mobile device through the screen, the speakers, or the vibrating component. As telerehabilitation systems are not mechanically hindering or guiding specific motions, the design of the most adequate Bio-Feedback methodology is not an easy task (Sigrist et al. 2013).

The Mobile Application. Data transmitted from different nodes are integrated into a mobile app, running on the Android-based device that also incorporates a visual interface, an auditive feedback generation module, and an auto-calibration and sensor data integration module. This interface will be presented in details in Section 5.

2.2 Physician Support Module

The proposed framework supports the physician during both the therapy definition and the telerehabilitation phase.

During the therapy definition, the physician is supported by a computer-assisted therapy definition software (Figure 1(c)) coupled with the sensing system (Figure 1(a)) in defining the sets of exercises for the telerehabilitation. In particular, the patient executes the rehabilitation exercises under the supervision of the physician, who defines the relevant physical ranges and reference execution speeds. The feedback subsystem can also be configured by the physician according to the specific exercise and patient needs.

During or after the telerehabilitation session, the physician can access the recorded data and visualize a set of desired variables as a 2D plot or as a 3D avatar, exactly reproducing the patient's limbs motions. Moreover, the physician can remotely adjust the therapy by changing the exercise series (order of execution of movements, number of repetitions, quality of execution goals, etc.).

2.3 Cloud Services

As shown in Figure 1(b), the cloud infrastructure, is in charge of managing all the services related to the definition, the execution, and the analysis of specific exercises for each patient. The main services the cloud could provide are:

- A set of tools to manage the archive containing all the possible exercises that the physicians can prescribe;
- A support tool to define and monitor the exercise set assigned to each patient;
- Storage support of all data coming from all the ReHapp instances. This module is in charge of managing a reliable and secure data transmission with the app, maintaining the whole storage available with backup/restore activities, and providing an interface for performing specific queries guaranteeing the correct privacy level;
- An analysis module to automatically evaluate the evolution of the rehabilitation path for a specific patient. This allows to highlight criticalities and trigger predefined alarms if critical situations arise;
- An inter-patient elaboration module to compare how different patients evolve in response to the prescribed rehabilitation therapies, to improve future rehabilitation and telerehabilitation practices; and
- Finally, in line with the current security policies, the communication involving patient, physician, and cloud-based services modules (see Figure 1) are characterized by the SSL encryption, and the access to the profile (for both patients and physicians) is protected by the username and a strong password (i.e., one that satisfies multiple criteria to be accepted).

3 THE SENSING SYSTEM

Motion tracking is becoming one of the most crucial arising tasks in general medicine, rehabilitation or even sports scenarios. When technology gets in contact with the human body, the system becomes inherently cyber-physical, since the characteristics of the human structure strongly affect the performance of the monitoring system and they must be taken into account to improve the precision of measurements and correctly reconstruct postures and actions. Most of the available solutions on the market are expensive, do not meet the medical requirements, or are too invasive to be autonomously used by the patient at his/her home (see Hadjidj et al. (2013) for a review of existing limb tracking systems).

The motion tracking system presented in this section is based on a set of low-cost wearable inertial measurement units (IMUs) coordinated as a wireless body area network. Body movements are tracked by integrating angular information acquired from a set of nodes, each monitoring a single rigid limb segment. The rest of this section presents the functional and technical requirements that had driven the hardware design and illustrates the various features of the platform.

3.1 Requirements

The sensing device has been designed according to a set of requirements derived from a tight interaction with physicians and therapists; the most crucial ones are reported below.

- **Resolution.** When monitoring body movements, a crucial aspect is to guarantee measurements with a given resolution, which depends on the monitored joint and the type of exercise. For example, in knee telerehabilitation applications, the flexion/extension angle must be typically monitored with an error below 1 degree.
- **Low-power consumption.** Sensor nodes should provide a good balance between lifetime and dimensions. In some applications is not possible to stop the activities to recharge the sensor or change batteries. However, large battery packs increase the overall sensor size and reduce the quality of the user experience.
- **Real-time processing.** If the monitoring system provides a feedback to the patient, or generates warning and alarm signals, then it is crucial to process data in real-time to guarantee a delay of approximately few hundred milliseconds between movement and visualization. In other applications, as sport training or gaming, such a delay may reduce to a few tens of milliseconds.
- **Configurability.** To avoid redesigning the sensing unit for slightly different applications, it is desirable that the platform is configurable to track, for example, different body parts, allowing different settings, such as sampling frequency, type of outputs (row data or quaternions), and online storage capabilities.
- **Usability.** Considering that sensors for rehabilitation are meant to be worn and used by inexperienced patients, they should be designed to be mounted easily and quickly on the body, in such a way they do not move during the execution of the exercises. Thus, comfort and wearability are important design objectives.

3.2 Hardware Platform

The sensing platform consists of a set of wearable nodes that send data to a central unit (master), which performs data integration to reconstruct the required information and visualize it in a proper form. In the current implementation, the central unit is a high-end system that runs the application under the Android operating system (Google 2014). The number of sensor nodes depends on the number of joints to be monitored. Figure 2 illustrates a block diagram of the main logical components in a node.

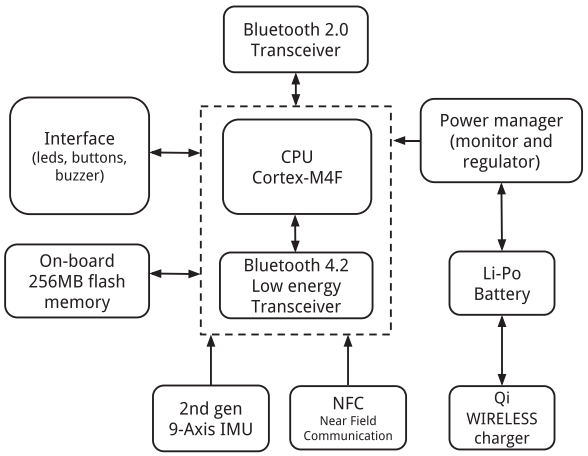

Fig. 2. Block diagram of the main node components.

Every node is operated by an ultra low-power Nordic nRF52822 microcontroller based on a 32-bit ARM Cortex-M4F CPU with 512kB flash and 64kB RAM, incorporating a rich selection of analog and digital peripherals, including a 2.4Ghz transceiver (Nordic Semiconductor 2015) that supports Bluetooth Low Energy (BLE) version 4.2, as well as 2.4GHz raw radio transmissions. The microcontroller is targeted for low-energy applications and supports several low-power operating modes, whose consumption ranges from 420nA in deep sleep to 5.5mA in RX mode.

The inertial measurements unit (IMU) is an InvenSense MPU-9250 that combines a 3-axis MEMS gyroscope, a 3-axis MEMS accelerometer, a 3-axis MEMS magnetometer, and a DMP hardware accelerator engine. The DMP acquires data from all sensors and computes the quaternion representing the chip orientation with respect to Earth fixed frame with a selectable output frequency up to 200Hz.

Aiming at simplifying the dressing procedure (avoiding the manual selection of the devices), the microcontroller has also been equipped with a Near Field Communication (NFC) peripheral. Exploiting a short distance information exchange, NFC technology enables a "touch-to-pair" functionality, allowing the user to connect a specific device by only putting it near the smartphone/tablet for a short period of time, during which the Bluetooth connection information and encryption keys are exchanged (NFCForum 2014). In this way, a node can be associated with a specific limb through a simple gesture and without knowing its network address.

The power supply is provided by a single cell LiPo battery that guarantees more than 40h of continuous use and can be charged using both USB or wireless recharge.

The device also features three LEDs, two buttons, and a buzzer for providing the user an auditory feedback. To comply with a specific requirement coming from the doctors and therapists, the power button requires a long-press to avoid accidental pressing, thus increasing the easy of use and functional robustness.

The case has been designed so that the sensor can be self mounted on a limb through an elastic band. The sensor includes a wireless charging module so that it can easily be recharged without cables putting it on its proper pad. The device weights about 30g and its dimensions are 4×3×0.8cm. The node's internal circuitry and the closed node are shown in Figure 3.

3.3 Software

In complex embedded devices like the one described in this section, the system must be able to execute several concurrent activities, some of which are subject to strict timing constraints, while

Fig. 3. The sensor node.

allowing a modular and flexible development cycle. For instance, IMU data are acquired with a sampling period that can be set between 5 and 20ms, while data transmission and data storage tasks can be triggered with a lower frequency and have lower criticality. For example, the data storage function is necessary to save motion data when the connection is not available.

To ensure a timely execution of the different activities and perform an off-line guarantee of the timing properties of the application, the software on the sensing module has been developed on top of the ERIKA Enterprise real-time kernel (Gai et al. 2000), which allows achieving high predictable timing behavior with a relatively small runtime overhead and memory footprint. On the used platform and kernel configuration context switch times are lower than 10ms and the kernel footprints is 1047 bytes.

3.4 Time Synchronization

In a sensing system like the one described in this article, the information of medical interest is reconstructed by integrating data samples received from different nodes of the network. To contain the error on the reconstructed joint angles, it is crucial to guarantee a timing coherence of the integrated samples, especially when monitoring dynamic physical variables, as in limb motion tracking. In fact, the amplitude of the error increases with the temporal misalignment among the samples to the signal.

Since the samples coming from different nodes can be received by the master node at different times, to correctly realign them, each data message has to be associated with a time stamp assigned at the acquisition time by the operating system running on the sensor node.

However, the time reference inside each node may differ due to local clock drift. Such a drift is due to several causes, including the poor quality of clock generators, possible variations in the supplied voltage, and changes of the environment temperature. For a given clock source, the maximum clock drift rate ξ_{sync} is expressed in parts per million (ppm). The typical accuracy found on commercial, low-quality, clock oscillators ranges from 40 to 80ppm (Syed and Heidemann 2006). For example, a clock with an accuracy of 40ppm produces a clock skew of 40ms per second. Given an operation time of an entire day, the resulting clock offset would result to be in the order of seconds.

Consider the example illustrated in Figure 4, where a joint angle is computed as the difference between two signals $f_1(t)$ and $f_2(t)$ produced by two corresponding nodes. As show in the figure, a time difference Δt in the node local clocks may produce an angular error θ_{err} proportional to the slope of the signals. In the worst case in which at time t the signals vary in opposite directions

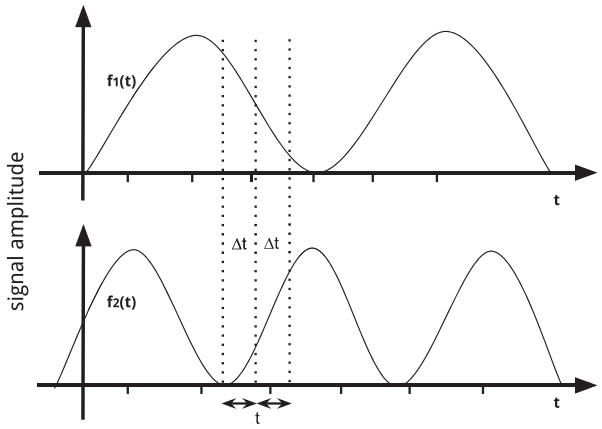

Fig. 4. Effect of time synchronization errors.

at the maximum speed ω_{max}, the angular error is given by

$$\theta_{err} = 2\omega_{max}\Delta t. \tag{1}$$

Considering that in a telerehabilitation scenario the angular speed of the knee joint is no greater than $\omega_{max} = 100$deg/s, and a measurement error $\theta_{err} = 1$deg is sufficient for the purpose, the maximum acceptable synchronization error results to be

$$\Delta t = \frac{\theta_{err}}{2\omega_{max}} = \frac{1\text{deg}}{200\text{deg/s}} = 5\text{ms}. \tag{2}$$

To contain the synchronization error, a clock synchronization algorithm is adopted to align local clocks on different nodes.

To run the synchronization protocol, a bandwidth reservation mechanism has been implemented on the sensor nodes (Marinoni et al. 2017), so that a fraction of the bandwidth is used by the nodes to send sampled data to the master using the BLE protocol (BT4 2014) and another fraction is used to exchange synchronization messages using a real-time protocol. The use of a second protocol is necessary, because the BLE does not provide support for timing guarantees and requires a multi-hop path for a communication between two non-master nodes. Moreover, not all devices provide an implementation of the full standard to reduce the footprint and power consumption. Typically, the companies producing the transceivers do not provide the code for the network stack, but only a library in binary format (e.g., Nordic SoftDevice (Nordic Semiconductor 2015)) that works as a black box. For this reason, a bandwidth reservation mechanism has been implemented to assign each node a slot of Q time units every P time units. Thus, P denotes the reservation *period*, while Q denotes the *budget* reserved in every period to real-time traffic.

To enable bandwidth reservation, some radio devices (as the Nordic, used in this article) provide a mechanism for using the radio device in raw mode in specific time slots, interleaved with the BLE traffic. Such time slots, however, are provided with a variable delay δ, which is necessary to complete the ongoing operation and release the radio device leaving the BLE protocol in a consistent state. Figure 5 shows an example of access sequence to the radio device by the two protocols.

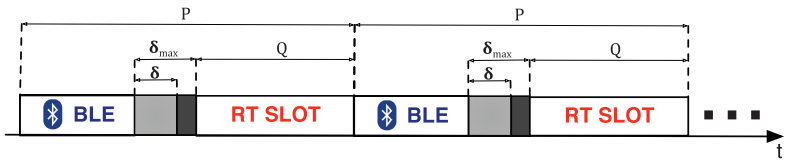

Fig. 5. Example of the protocols access sequence to the radio.

3.5 Sensing Nodes Coordination

The proposed approach is centralized regarding both the network topology and the estimation algorithm.

The network topology is organized as a star, as mandated by version 4.x of the BLE protocol, which also limits the maximum number of nodes to seven peripheral slaves plus a central device master. Note that such limitations can be relaxed with the upcoming version 5.0 of BLE, which allows adopting a mesh topology with a higher number of nodes.

The estimation algorithm has been designed according to a centralized approach, taking into account the star topology imposed by the BLE 4.x protocol. In fact, a distributed solution would less effective due to an increased network traffic, overhead, and delay. Having identical nodes also simplifies the system development and its usage (i.e., a node is assigned to a limb during the dressing phase). Moreover, performing only the sensing part in the node allows reducing cost, weight, and energy consumption. One of the problems of making the algorithm fully distributed is that nodes located on different limbs could require specific software modules and a proper underlying infrastructure must be provided to maintain the flexibility in the user experience. A possible solution for managing a distributed implementation could be designing the framework based on the multi-agent paradigm (Calvaresi et al. 2017b). However, the advantages of a distributed estimation algorithm concerning cost, size, weight, battery consumption, and so on, strongly depend on the application scenario that must be analyzed individually.

Regarding performance of the current solution, the maximum sampling frequency depends on the BLE throughput and the number of connected nodes. Multiple BLE connection parameters affect the throughput, but the most important one is the Connection Interval, which defines how often a BLE communication will occur. According to the BLE specification, the minimum valid Connection Interval is 7.5ms. There can be a maximum of six packets sent in each Connection Interval, and the packet payload has a limit of 20 bytes.

Therefore, the maximum BLE throughput can be computed as

$$Throughput = \frac{6 * 20\text{bytes}}{7.5 * 10^{-3}\text{s}} = 128\text{kb/s}. \tag{3}$$

Considering that each sample transmitted by a node fits in a single BLE packet (20 bytes), each node requires a bandwidth of 16kb/s. Hence, the maximum number of nodes sampling at a frequency of 100Hz is 128/16 = 8, which is above the limit imposed by the current topology.

4 ANATOMICAL JOINT ESTIMATION AND TRACKING ALGORITHM

Monitoring the articular joints during rehabilitation requires the integration of the data produced by the nodes located on the patient limbs. Each node provides the raw data acquired from the IMU and an attitude information through a quaternion, representing the rotation of the frame attached to the sensor (sensor frame) with respect to a reference frame (Earth frame) (Mahony et al. 2008; Madgwick et al. 2011). Compared to other techniques, like rotational matrix and Euler Angles, quaternions improve computational efficiency and avoid singularities problems (e.g., gimbal lock).

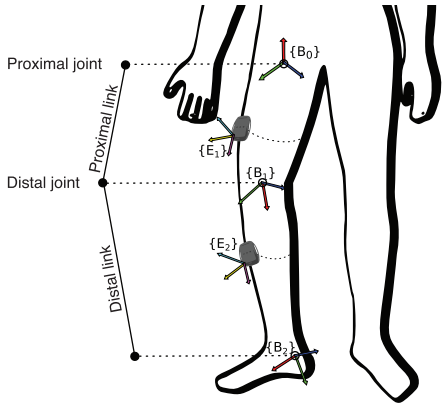

Fig. 6. Anatomical frames positioning and sensors wearing on the leg.

Since raw data coming from the IMU are highly corrupted by noise, drift, and tissue artifacts (Tehrani 1983; El-Sheimy et al. 2008; Leardini et al. 2005), a proper filtering technique is essential for achieving a posture estimation. Besides, measurements are related to the sensor frame, which is translated and rotated with respect to the ideal articular joint frame: considering the structural differences between patients and the manual procedure for positioning the sensors, such frame displacement is in general unknown. Many approaches in the literature leave this issue unsolved (El-Gohary and McNames 2012; Yun and Bachmann 2006; Zhang et al. 2011).

This section describes a self-calibration algorithm that exploits the kinematics constraints of the human articular structure (Seel et al. 2014) to estimate the orientations of the knee joint, modeled as a rotoidal hinge joint. The estimation phase requires the patient to perform some general movements that are used to identify the position of the joint axes. While the joint tracking algorithm is performed using quaternions, the kinematic joint estimator is developed using the raw data produced by the IMU, due to the unknown attitude of the sensors. Each inertial sensor is assumed to be rigidly connected to a different body link, as depicted in Figure 6.

We denote:

—$\{F\}$ as the inertial earth-fixed-frame reference;
—$\{E_s\}$, $s = 1, \ldots, S$ as the sensor-fixed-frame reference;
—$\{B_i\}$, $i = 1, \ldots, I$ as the articular joint-fixed-frame reference.

Limbs articulations are approximated as spheroidal or rotoidal joints assuming that the frames $\{B_i\}$ and $\{B_{i+1}\}$ are kinematically constrained and the articular link between assumes the notation $\{L_{i+1}\}$.

4.1 Knee Joint Axes Estimation Algorithm

The kinematic constraints of the knee joint are used to estimate the direction and the position of the knee flexion/extension axis in the local frames of the sensors attached to the upper leg and the lower leg ($\{E_1\}$ and $\{E_2\}$, respectively). The nodes located to the limbs provide the acceleration vectors $\mathbf{a}_1(k), \mathbf{a}_2(k) \in \mathbb{R}^3$ and angular speeds around the sensor frame axes $\boldsymbol{\omega}_1(k), \boldsymbol{\omega}_2(k) \in \mathbb{R}^3$, where k is the discrete time. Position and orientation of the inertial sensors on the respective links are assumed to be unknown.

The algorithm uses a training data set to estimate the versors $\boldsymbol{v}_1$ and $\boldsymbol{v}_2 \in \mathbb{R}^3$ of the flexion/extension axis of the knee in the local sensor frames. Note that $\boldsymbol{v}_1$ and $\boldsymbol{v}_2$ are constant and

only depend on the orientation of the IMUs with respect to the joint (Seel et al. 2014). Since sensors are not rigidly attached to the bones, disturbances are due to the soft tissue artifact (Leardini et al. 2005; Peters et al. 2010). In this work, this issue is not addressed, because the accuracy typically reached in the estimation of kinematic joints has the same order of magnitude of the tissue artifacts.

The angular rates $\boldsymbol{\omega}_1(k), \boldsymbol{\omega}_2(k)$ of the gyroscopes expressed in the joint frame $\{E_1\}$ and $\{E_2\}$, respectively, depend only by a time-variant rotation matrix and the knee joint angle rate. Considering that the projection of the gyroscopes angular rates $\boldsymbol{\omega}_1(k), \boldsymbol{\omega}_2(k)$ on the plane normal to the joint axis have the same amplitude at each time, we can write that

$$\|\boldsymbol{\omega}_1(k) \times \boldsymbol{v}_1\|_2 - \|\boldsymbol{\omega}_2(k) \times \boldsymbol{v}_2\|_2 = 0 \quad \forall k. \tag{4}$$

Note that Equation (4) holds regardless of the inertial sensors position and orientation. To estimate versors $\boldsymbol{v}_1$ and $\boldsymbol{v}_2$, Equation (4) is used to define a minimization problem following the approach in Seel et al. (2014). Therefore, replacing $\boldsymbol{v}_1$ and $\boldsymbol{v}_2$ with their estimation $\hat{\boldsymbol{v}}_1$ and $\hat{\boldsymbol{v}}_2$ the following estimator function is obtained:

$$\|\boldsymbol{\omega}_1(k) \times \hat{\boldsymbol{v}}_1\|_2 - \|\boldsymbol{\omega}_2(k) \times \hat{\boldsymbol{v}}_2\|_2 = e(k) \quad \forall k, \tag{5}$$

where $e(k)$ is the error that should be minimized. To obtain a proper estimation of the versors $\hat{\boldsymbol{v}}_1$ and $\hat{\boldsymbol{v}}_2$, a coordinate transformation from cartesian to spherical representation is performed with unitary radial distance as

$$\begin{aligned} \hat{\boldsymbol{v}}_1 &= [\cos\hat{\phi}_1 \cdot \cos\hat{\theta}_1,\ \cos\hat{\phi}_1 \cdot \sin\hat{\theta}_1,\ \sin\hat{\phi}_1\,], \\ \hat{\boldsymbol{v}}_2 &= [\cos\hat{\phi}_2 \cdot \cos\hat{\theta}_2,\ \cos\hat{\phi}_2 \cdot \sin\hat{\theta}_2,\ \sin\hat{\phi}_2\,], \end{aligned} \tag{6}$$

where $\hat{\phi}_i$ and $\hat{\theta}_i$, $i = 1, 2$ are the elevation and azimuth angles, respectively.

By defining the state as $\boldsymbol{\chi} = [\hat{\phi}_1,\ \hat{\theta}_1,\ \hat{\phi}_2,\ \hat{\theta}_2]$, the function to be minimized can be expressed as

$$\underset{\boldsymbol{\chi}}{\text{minimize}} \quad \sum_{k=1}^{N} e^2(k). \tag{7}$$

The cost function in Equation (7) has four minima that correspond to the sign combinations. This work follows the approach proposed in Seel et al. (2014) to find the correct combination of signs. The minimization problem expressed in Equation (7) can be solved by a gradient descent algorithm, like BFGS or Newton's methods (Gill et al. 1981; Kelley 1999).

Once the knee joint axis direction is identified in both the sensor frames, the flexion/extension knee angle can be computed. As specified in Figure 7, the IMUs provide a stable estimation of the quaternions representing the orientation of each sensor with respect to the fixed reference frame. In this approach, the knee flexion/extension angle β_{fe}^{knee} is computed as

$$\beta_{fe}^{knee} = \sphericalangle_{3d}(\hat{\boldsymbol{R}}_1(k) \cdot (\hat{\boldsymbol{v}}_1 \times \boldsymbol{c}), \hat{\boldsymbol{R}}_2(k) \cdot (\hat{\boldsymbol{v}}_2 \times \boldsymbol{c})), \tag{8}$$

where $\sphericalangle_{3d}$ is the angle between two vectors in three-dimensional space and $\hat{\boldsymbol{R}}_1(k)$ and $\hat{\boldsymbol{R}}_2(k)$ are the rotation matrices provided by the two IMUs, respectively.

5 USER INTERFACE

The user interface has been implemented as an Android application, named ReHapp, developed with the aim of supporting patients and doctors during rehabilitation sessions. It helps patients during the execution of the exercises, as well as doctors and therapists in prescribing activities to patients and evaluating their performance.

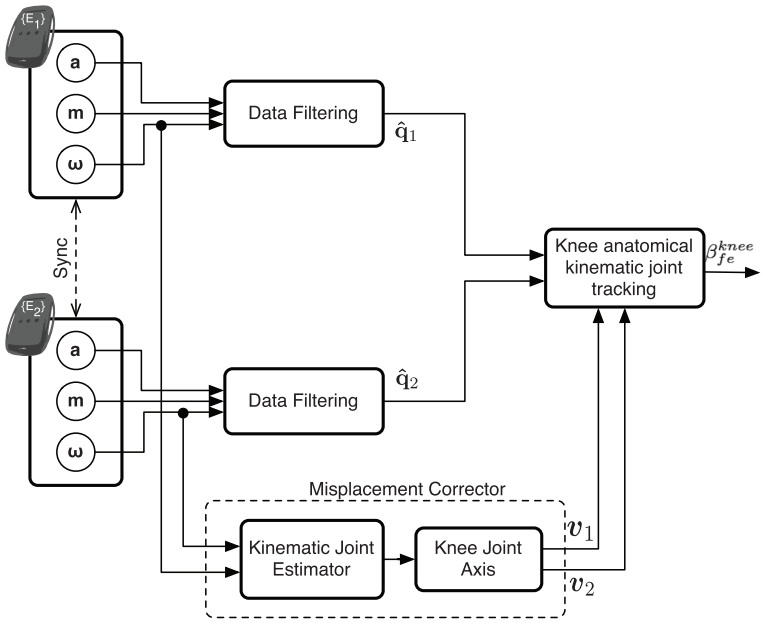

Fig. 7. Block diagram of the joint estimation and tracking algorithm.

During the rehabilitation sessions, patients are supported by a 2D graphics, as well as by a 3D human avatar. The 2D graphics shows the angular values of the knee joint in real time and visualizes the discrepancy between the pre-stored trace and the movements measured by the sensors during the exercise. Once the session is concluded, statistics are reported and stored. The more intuitive 3D Avatar is used at the beginning to show the precise series of movements to be executed. Moreover, it replicates the actual patients' actions during the exercise.

The app also provides a real-time audio feedback to inform the patient about the quality of the execution performance. Such an audio feedback plays the role of a "therapeutic evaluation," which is very helpful to increase the patient motivation. Normally, in fact, after the first days at home without a guide the motivation drops, as well as the number and the quality of the exercises carried out.

The features of the app are presented below, illustrating how the users can interact with it.

5.1 Selecting and Executing An Exercise

Before starting a rehabilitation session, both the patient and the exercise must be selected. By tapping a specific button on the main screen, a dialog with the list of registered patients is displayed. When selecting a patient, the list of the exercises entered by the therapist is presented. For each exercise the therapist can specify the type of exercise, the range of extension, the number of repetitions of the movements and how many times the exercise should be repeated. Once the desired exercise is selected, the patient is ready to start the rehabilitation session supported by the interface depicted in Figure 8.

The human-like 3D avatar visualized on the left-hand side (a) can be positioned in one of the predefined configurations (e.g., sitting, standing), depending on the selected exercise, and replicates the movements of the monitored limbs. The interface on the right-hand side has the purpose

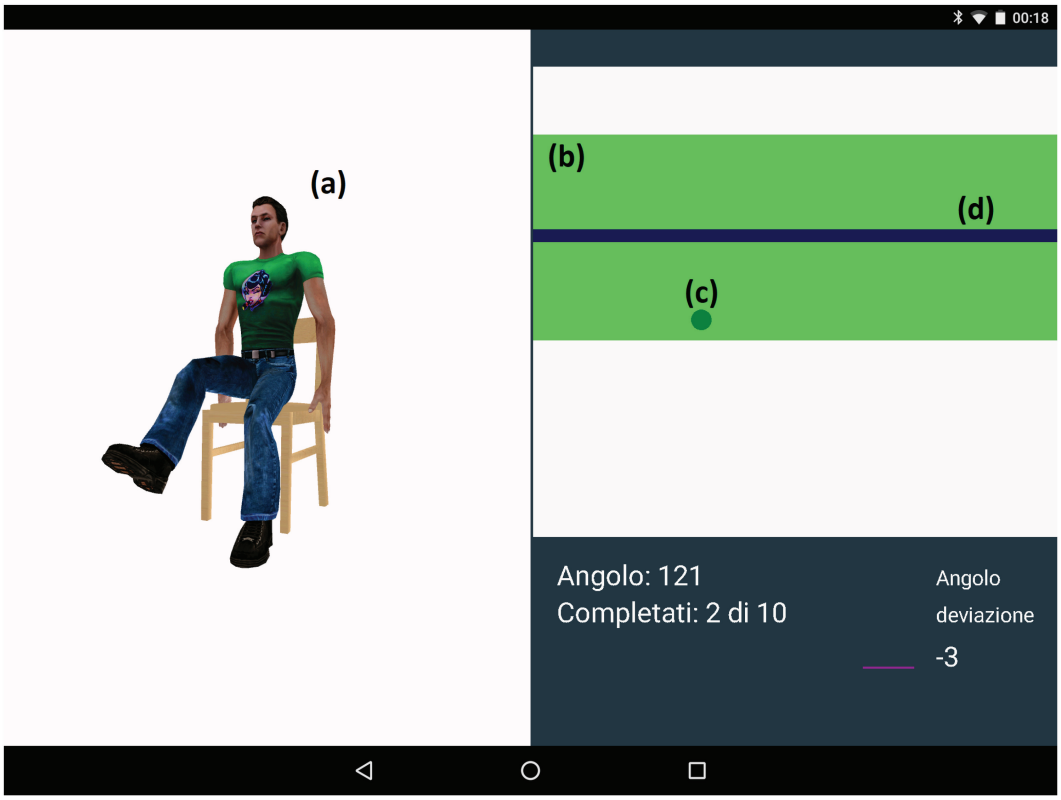

Fig. 8. Screenshot related to a specific exercise execution.

of guiding the patient in correctly performing the movements requested by the current exercise. In particular, referring to Figure 8:

— The area denoted by (b) indicates (vertically) the range within which the knee angle should stay during the exercise;
— The dark dot (c) shows the target reference value that has to be reached to complete the current movement;
— The horizontal line (d) indicates the current angular position and translates up and down following the movements performed by the patient.

5.2 Statistics

At the end of the session, ReHapp enables the visualization of patient's performance and results. After selecting the desired patient from the list, the screen shown in Figure 9 is displayed. For every saved exercise, three bars with different colors are displayed:

— The blue bar (a) represents the number of correctly performed repetitions, that is, the ones where the patient successfully reached the maximum and the minimum extensions;
— The yellow bar (b) represents the number of repetitions in which the patient exceeded the prescribed extension range while staying within the tolerance range;
— The red bar (c) represents the number of repetitions in which the patient exceeded both the prescribed extension range and the tolerance range.

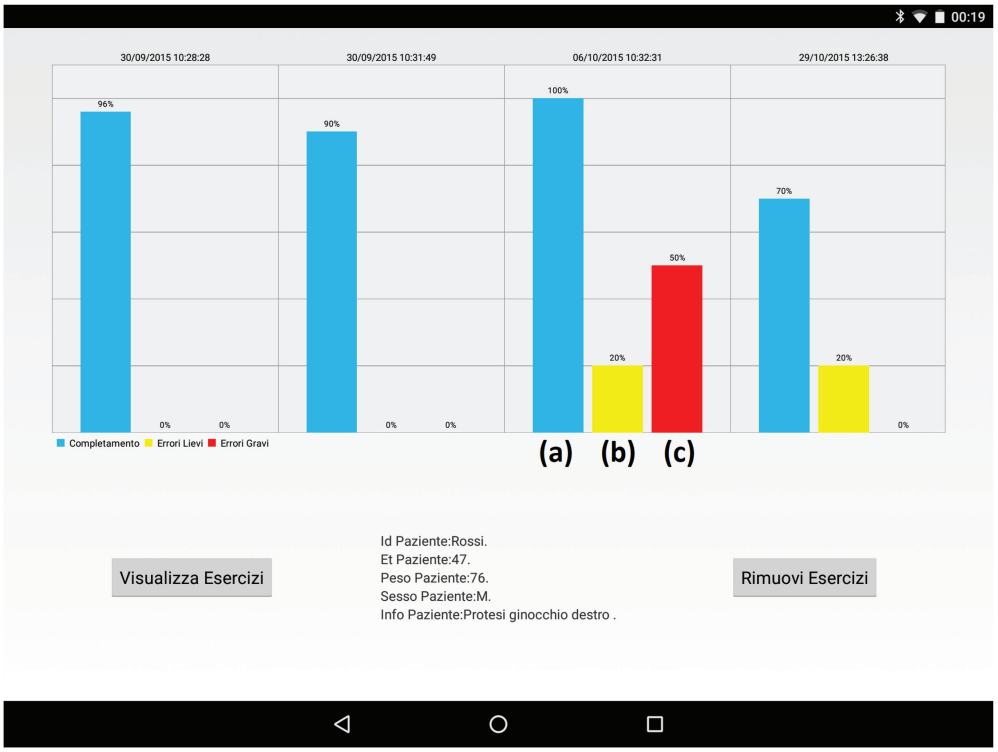

Fig. 9. Screen of the statistics of the recorded exercises.

By selecting a specific exercise, the screen shown in Figure 10 is displayed. The interactive plot contains all recorded angles of the knee extension during the exercise, the prescribed range and, on the bottom side of the screen, a report with statistics.

6 EXPERIMENTAL RESULTS

This section presents some experimental results carried out to evaluate the effectiveness of the sensing system in measuring orientations and providing timely data. Furthermore, a set of tests is presented for validating the kinematic anatomical joint estimation algorithm. Finally, a preliminary feedback is reported from a clinical trial in progress in a rehabilitation center.

6.1 Orientation Accuracy

The orientation errors of the sensor node were evaluated with respect to a reference given by a Polhemus Patriot system (Polhemus 2010), which provides the position and orientation of a mobile probe with respect to a fixed reference station. In particular, the fixed reference station emits a tuned electromagnetic field that is measured by the mobile probe. This procedure avoids performing hybrid data merging via software. The resulting resolution is about 0.03mm and 0.01 degrees, whereas the static accuracy is of 1.5mm RMS for the position and 0.4 degrees RMS for the orientation.

In the performed test, both the Polhemus and the inertial sensor node have been mounted on a rotating link, as illustrated in Figure 11(a), to avoid any measurement error caused by misalignments.

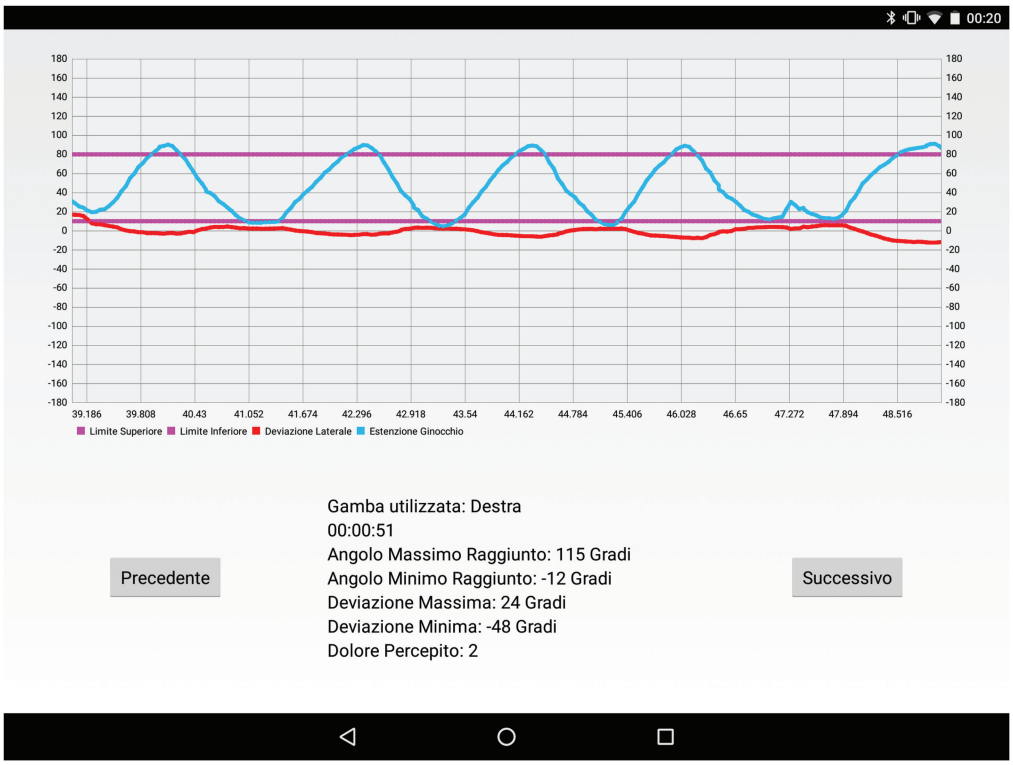

Fig. 10. Detailed statistics for a specific recorded exercise.

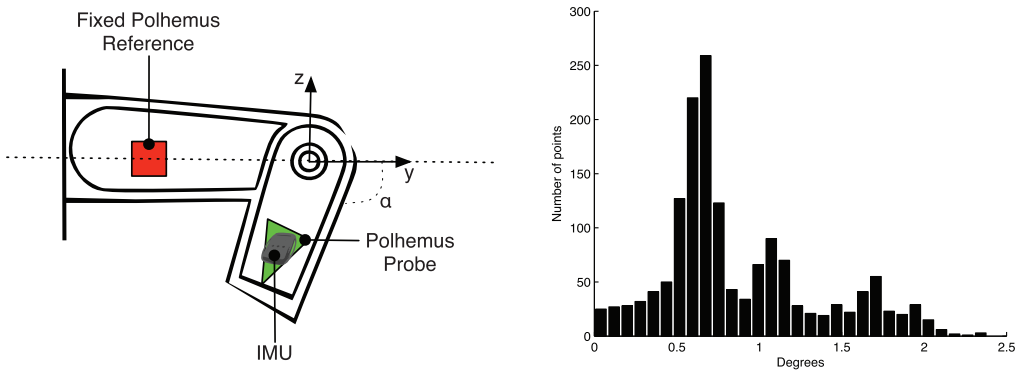

(a) (b)

Fig. 11. (a) Experimental setup used to evaluate the sensor accuracy; (b) Distribution of the angular error.

The orientation accuracy of the sensor node was measured by converting quaternions to Euler angles and directly comparing them to the ones given by the Polhemus. Only the angles around X and Y axes were measured, because rotations around the Z axis rely on magnetometers, which are strongly affected by the magnetic field generated by the Polhemus.

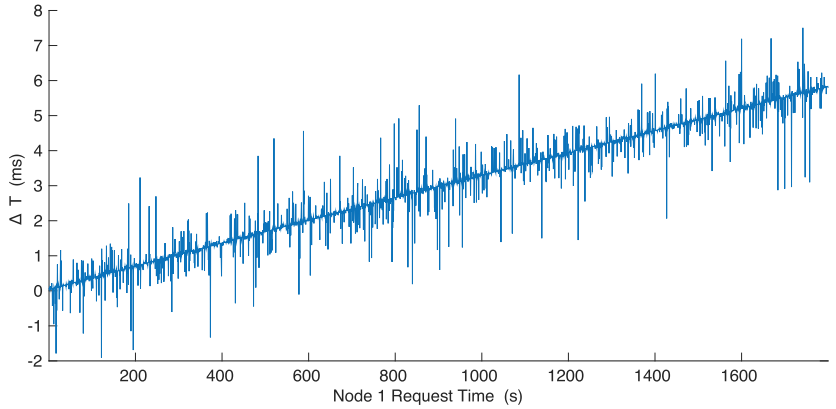

Fig. 12. Drift between slot requests performed by two nodes with initial synchronization only.

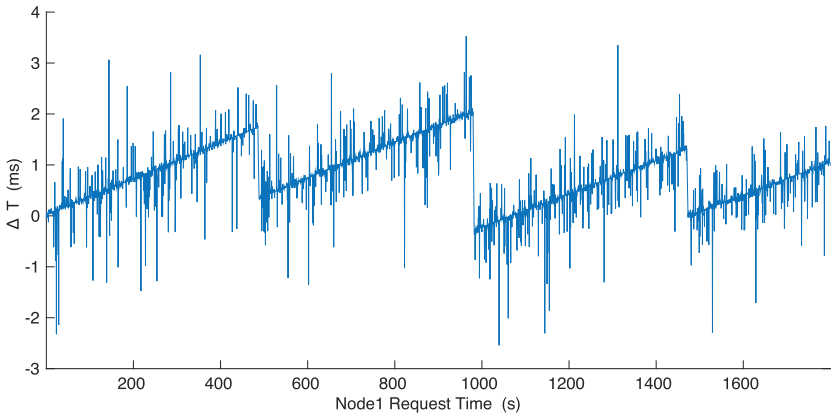

Fig. 13. Drift between slot requests performed by two nodes when the synchronization is repeated every 8min.

Figure 11(b) shows the IMU measurement error distribution with respect to the Polhemus reference. Note that the error mean is 0.8685 degrees and its RMS is 0.9871 degrees. Considering the lower cost of the inertial sensor with respect to the Polhemus (i.e., tens of euros compared to thousands of euros) the achieved results are quite satisfactory.

6.2 Synchronization Error Evaluation

A set of experiments has been performed to test the effectiveness of the clock synchronization protocol described in Section 3.4 to align local clocks within a desired error. These tests have been carried out using two nodes: each node notifies its requests on a digital output and requests from both nodes are acquired with a logic analyzer to make the measurement error negligible.

In the first experiment, the nodes execute the synchronization procedure during the initialization phase and then operate for an interval of 30min without re-synchronizing their clocks. Figure 12 shows that the relative clock error (ΔT) increases linearly, as expected, thus justifying the need for a synchronization protocol.

In the second experiment, nodes were synchronized with a period $P_{sync} = 8$min. Figure 13 shows the relative clock error of the two nodes. As clear from the plot, the synchronization protocol can

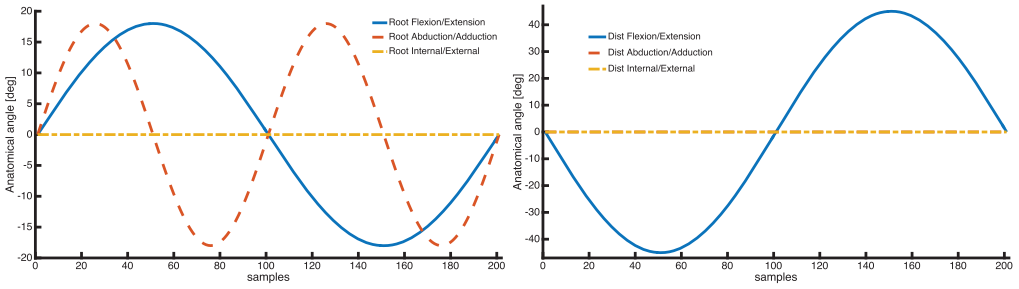

(a) (b)

Fig. 14. Anatomical joint motion imposed to the stick model: (a) flexion/extension, abduction/adduction and internal/external angles position of Root joint; (b) flexion/extension, abduction/adduction and internal/external angles position of Distal joint.

bound the drift by a constant that depends on the drift rate, the synchronization period, and the execution time of the SoftDevice interrupt routine. With the adopted experimental configuration, the measured synchronization error fully respects the constraint given by Equation (2) in Section 3.4. Note that the spikes are caused by the execution delay of the timer interrupt handler, which prevents the synchronization protocol to totally reset the clock error between the two nodes. However, such an error does not affect the accuracy of the measurements, which only requires a bound on the maximum value of the drift.

6.3 Joint Angle Estimation

To show the effectiveness of the anatomical joint estimation algorithm presented in Section 4, a simulation test has been performed by imposing a combination of sinusoidal movements to a mannequin for replicating the motion of the proximal and distal links of the leg. In this way, leg movements are completely defined and known in the anatomical frames described in Figure 6. The IMUs measure the motion inducted to their respectively frame and by means of gyroscopic data.

Two seconds of movements were simulated and sampled at 100Hz: the position of the proximal link is identified by the frame $\{B_0\}$ and the distal one is identified by $\{B_1\}$.

Figure 14(a) depicts the set of flexion/extension, abduction/adduction, and internal/external rotation angle positions, with respect to the time samples, imposed to the joint frame $\{B_0\}$ and relative to the proximal link $\{L_1\}$ defined in Figure 6. Figure 14(b) shows the set of rotation angle positions for the distal joint $\{B_1\}$. As clearly visible from the plot, only the flexion/extension has non zero values, compatibly with a knee joint.

The motion performed by the mannequin is captured as angular velocities measured by the IMU's gyroscopes. Figure 15(a) depicts the angular velocities measured by the IMU gyroscope $\{E_1\}$ attached to link $\{L_1\}$ around its axes ω_α, ω_β, and ω_γ. Figure 15(b) depicts the angular velocities measured by the IMU gyroscope $\{E_2\}$ attached to link $\{L_2\}$ around its axes ω_α, ω_β, and ω_γ.

The minimization of the functional given in Equation (7) is obtained by a Newton's method in less than 20 iterations as shown in Figure 16. Each state element converges to the real value highlighted by the diamonds in the graph. The estimation algorithm requires that the initial movements stimulate the gyroscopes in all directions to avoid non-observable states and ill-conditioned data matrices.

Once the estimation of $\hat{\boldsymbol{v}}_1$ and $\hat{\boldsymbol{v}}_2$ is performed, the knee flexion/extension angle tracking can be performed according to the procedure depicted in Figure 7 and described in Section 4.1. From the

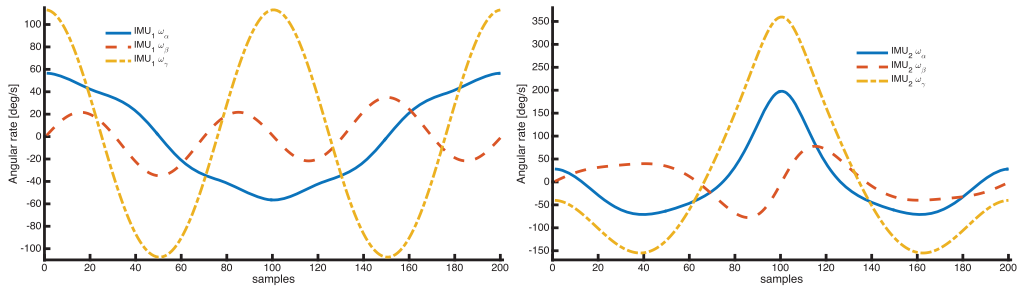

Fig. 15. Angles rates of 3-axis gyroscopes: (a) sensor attached to link L_1 with reference frame E_1; (b) sensor attached to link L_2 with reference frame E_2.

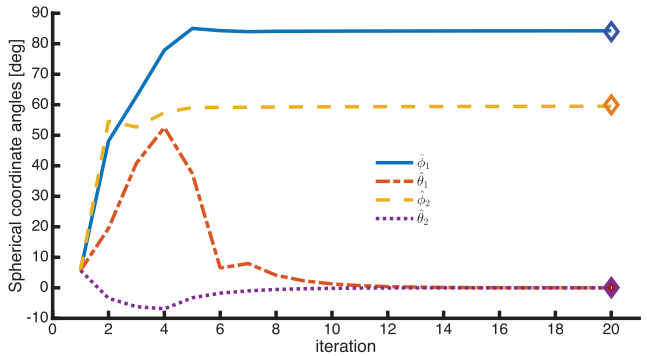

Fig. 16. Spherical coordinates $\hat{\phi}_1$, $\hat{\theta}_1$, $\hat{\phi}_2$, $\hat{\theta}_2$ of the knee joint as a function of the estimation algorithm iterations.

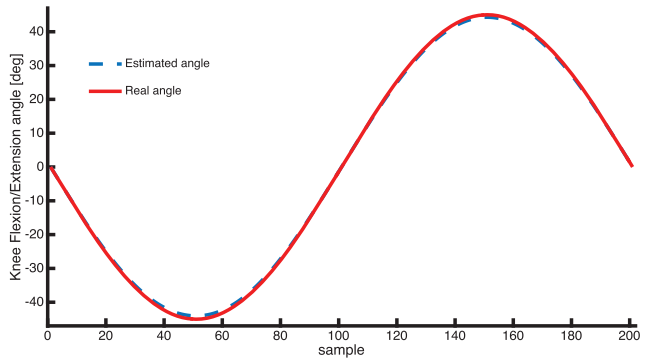

Fig. 17. Estimated flexion/extension knee angle compared with the actual value.

estimated quaternions $\hat{\boldsymbol{q}}_1$ and $\hat{\boldsymbol{q}}_2$ and knee joints directions $\hat{\boldsymbol{v}}_1$ and $\hat{\boldsymbol{v}}_2$, the knee flexion/extension estimation is obtained by Equation (8) with a very high accuracy, as shown in Figure 17.

6.4 Clinical Validation

The presented platform has been validated in a clinical trial carried out at the "Versilia" Hospital in Viareggio, Italy, aimed at evaluating the system performance and usability. Such a trial started

in September 2015 and lasted one year, providing support to doctors and therapists to keep track of patients, exercises, and improvements.

To provide significant outcomes, the trial was designed to involve at least 50 patients for about two months each. Balancing the men/women composition, the patients have been properly selected by the medical personnel, among those who experienced a total knee replacement.

To provide a framework supporting the telerehabilitation best practices, the whole process (system design, and development) has been carried out in continuous collaboration with medical practitioners, therapists, and caregivers. This approach allowed refining and tailoring functional and non-functional requirements to different operating scenarios.

A subset of 28 out of 50 patients have been interviewed in a post-trial system evaluation, together with the medical staff involved in this study. The patients were asked to fill a detailed online questionnaire to evaluate the expectations, the functionality, and the overall experience. At the end, the potential benefits, already manifested by the patients in a preliminary evaluation of the system, have been confirmed. Patients and physicians unanimously agreed in confirming that all the requirements defined for the system under evaluation have been met. Aiming at guaranteeing the patients anonymity, the outcomes have been summarized as follows.

Regarding the patients' experience, the most appreciated features have been:

- *Auto-calibration:* Considering patients who experienced the system with and without the sensors auto-calibration, an extremely positive feedback have been recorded for such a feature;
- *User-interface:* Performing repeatedly (and sometimes painful) movements for several minutes can be discouraging and boring. However, having such a stimulating interface made those minutes/hours of therapy flew away;
- *Small nodes size:* the small dimensions of the sensors and the wireless technology has not been perceived too cumbersome during the therapy execution;
- *Nodes wearability:* No complex setups are required. Hence, in a few simple steps the sensors are in place and ready to work.

Concerning the medical staff, the relevant outcomes have been:

- *Long-press functionality:* It has ensured that no unintentional button presses could hamper the session anyhow;
- *Auto-calibration:* It has simplified the wearing phase, ensuring data correctness even in the presence of sensors misplacement;
- *Battery life-time:* The autonomy of more than 48h (with data streaming at 100Hz) made possible to continuously monitor patients without any annoying interruption for changing/recharging the sensors and preventing data loss due to sudden energy interruption;
- *Measure accuracy:* It has been considered satisfactory and beyond medical expectations, thus enabling detailed analysis and better understanding;
- *Follow-up boost:* The proposed system fastened the process of recording and adapting patients therapies;
- *Monitoring boost:* The possibility to analyze both raw and pre-elaborated data allowed creating historical data supporting the decision-making process in future diagnosis and therapy definition/adaption/suspension.
- *Therapy adherence:* The central role of the patients in the rehabilitation process made them more responsible and proactive during the therapy. Moreover, having an intuitive real-time feedback as a 3D avatar worked as an extremely motivating factor for improving their performance.

Finally, ReHapp has been presented at a national fair on ICT for disabilities[1] and received positive comments by both users and rehabilitation practitioners on the intuitiveness of the user interface.

7 CONCLUSIONS

This article presented a CPS framework for supporting patients and therapists in the setup, execution, and evaluation of exercises required for rehabilitation purposes, experimented and validated for the case of knee telerehabilitation.

The work highlighted interesting cyber-physical design challenges originated by the tight interaction of the monitoring system with *(i)* the physical characteristics of the monitored body limbs (inner loop, patient-tablet) and *(ii)* the physician platform guiding the rehabilitation process (outer loop, patient-physician). As shown in the article, dealing with the kinematic constraints of the human body allows achieving not only a significant reduction of the errors in the sensor measurements but also a compensation of the uncertainties due to the imprecise positioning of the sensors on the limbs. In addition, a joint estimation algorithm has been proposed to derive a self-calibration procedure that can easily be performed by patients during a setup phase to increase the robustness of the measurements. A possible direction to further improve the sensor nodes involves the use of upcoming devices embedding support for the new version 5.x of the Bluetooth Low Energy protocol. In this way, it will be possible to adopt less restricted network topologies and remove the limitations in term of the number of nodes.

A crucial component of the proposed system is represented by the wearable sensor, purposely designed to balance cost, accuracy, energy-consumption, real-time processing, and simple interface to comply with the requirements specified by the therapists and overcome the actual limitations of the sensors existing on the market. Accuracy in the reconstructed motion is also achieved thanks to a dual-protocol communication support, which has been developed to combine BLE data transmissions towards a mobile device with an intra-node real-time communication used for synchronizing local clocks to reduce time drifts and align data samples in time.

The achieved results, including the clinical trial, have been extremely encouraging and in line with the initial expectations. The feedback received from physicians and patients during the trial offered interesting insights to improve the functionality of the app and further enhance the entire system. For instance, the graphical user interface, perceived as a simple videogame, could be further improved toward providing a gamification path to improve the patients' experience. Currently, a follow-up of the trial is under evaluation to test the cloud-based component of the framework and the related synergies of the outer feedback loop.

The presented framework has been considered by Calvaresi et al. (2017b) to propose an agentification of the platform to improve its functionality, and flexibility, thus proving its general suitability for targeting a broader set of stakeholders requiring physical (e.g., hip, shoulder, neck, and back) or cognitive (e.g., post stroke or traumatic brain injury) rehabilitation. The presented framework is also expected to be employed for pre-frailty assessment (Gill et al. 2002). Finally, non-biomedical scenarios (e.g., beach tennis, golf, biking, curling) can be also addressed by the proposed approach. Since regulated by less stringent safety normative, the main challenge in these applications is to focus on the user interface to enhance the user experience.

ACKNOWLEDGMENTS

The authors thank the Telecom Italia White JOL for providing specifications about the application scenario and Dott. Posteraro from Ospedale "Versilia" for fruitful discussion and clinical support.

[1] HANDImatica2014, Bologna, Italy, organized by ASPHI.

REFERENCES

Flavia Benettazzo, Sabrina Iarlori, Francesco Ferracuti, Andrea Giantomassi, Davide Ortenzi, Alessandro Freddi, Andrea Monteriù, Silvia Innocenzi, Marianna Capecci, Maria Gabriella Ceravolo, and Sauro Longhi. 2014. Low cost RGB-D vision based system to support motor disabilities rehabilitation at home. In *Proceedings of Ambient Assisted Living: Italian Forum*.

Bluetooth Specification Version 4.2. 2014. Retrieved from https://www.bluetooth.org/en-us/specification/adopted-specifications.

Pasquale Buonocunto and Mauro Marinoni. 2014. Tracking limbs motion using a wireless network of inertial measurement units. In *Proceedings of the 9th IEEE International Symposium on Industrial Embedded Systems (SIES'14)*.

Davide Calvaresi, Daniel Cesarini, Mauro Marinoni, Paquale Buonocunto, Stefania Bandinelli, and Giorgio Buttazzo. 2015. Non-intrusive patient monitoring for supporting general practitioners in following diseases evolution. In *Proceedings of the 3rd International Conference on Bioinformatics and Biomedical Engineering (IWBBIO'15)*.

Davide Calvaresi, Daniel Cesarini, Paolo Sernani, Mauro Marinoni, Aldo Franco Dragoni, and Arnon Sturm. 2017. Exploring the ambient assisted living domain: A systematic review. *J. Ambient Intell. Human. Comput.* 8, 2 (2017), 239–257.

Davide Calvaresi, Andrea Claudi, Aldo Franco Dragoni, Eric Yu, Daniele Accattoli, and Paolo Sernani. 2014. A goal-oriented requirements engineering approach for the ambient assisted living domain. In *Proceedings of the 7th International Conference on Pervasive Technologies Related to Assistive Environments*. ACM, 20.

Davide Calvaresi, Mauro Marinoni, Arnon Sturm, Michael Schumacher, and Giorgio Buttazzo. 2017a. The challenge of real-time multi-agent systems for enabling IoT and CPS. In *Proceedings of IEEE/WIC/ACM International Conference on Web Intelligence (WI'17)*. DOI: http://dx.doi.org/10.1145/3106426.3106518

Davide Calvaresi, Michael Schumacher, Mauro Marinoni, Roger Hilfiker, Aldo Franco Dragoni, and Giorgio Buttazzo. 2017b. Agent-based systems for telerehabilitation: Strengths, limitations and future challenges. In *Proceedings of the 10th Workshop on Agents Applied in Health Care (A2HC'17)*.

Daniel Cesarini, Pasquale Buonocunto, Mauro Marinoni, and Giorgio Buttazzo. 2014. A telerehabilitation framework for lower-limb functional recovery. In *Proceedings of International Conference on Body Area Networks (BodyNets'14)*.

Daniel Cesarini, Davide Calvaresi, Chiara Farnesi, Diego Taddei, Stefano Frediani, Bodo E. Ungerechts, and Thomas Hermann. 2016. MEDIATION: An eMbEddeD system for auditory feedback of hand-water InterAcTION while swimming. *Procedia Eng.* 147 (2016), 324–329.

Daniel Cesarini, Davide Calvaresi, Mauro Marinoni, Paquale Buonocunto, and Giorgio Buttazzo. 2015. Simplifying telerehabilitation devices for their practical use in non-clinical environments. In *Proceedings of the 3rd International Conference on Bioinformatics and Biomedical Engineering (IWBBIO'15)*.

Rory A. Cooper, Shirley G. Fitzgerald, Michael L. Boninger, David M. Brienza, Nigel Shapcott, Rosemarie Cooper, and Katherine Flood. 2001. Telerehabilitation: Expanding access to rehabilitation expertise. *Proc. IEEE* 89 (Aug. 2001), 1174–1193.

Mahmoud El-Gohary and James McNames. August 2012. Shoulder and elbow joint angle tracking with inertial sensors. *IEEE Trans. Biomed. Eng.* 59 (Aug. 2012), 2635–2641.

Naser El-Sheimy, Haiying Hou, and Xiaoji Niu. 2008. Analysis and modeling of inertial sensors using allan variance. *IEEE Trans. Instrument. Measure.* 57 (2008), 140–149.

Paolo Gai, Giuseppe Lipari, Luca Abeni, Marco di Natale, and Enrico Bini. 2000. Architecture for a portable open source real-time kernel environment. In *Proceedings of the 2nd Real-Time Linux Workshop and Hand's on Real-Time Linux Tutorial*.

Andrea Giantomassi, Marianna Capecci, F. Benettazzo, Sabrina Iarlori, Francesco Ferracuti, Alessandro Freddi, Andrea Monteriù, Silvia Innocenzi, Paola Casoli, Maria Gabriella Ceravolo, Sauro Longhi, and Tommaso Leo. 2014. Training and retraining motor functions at home with the help of current technology for video games: Basis for the project. In *Proceedings of Ambient Assisted Living: Italian Forum*.

Philip E. Gill, Walter Murray, and Margaret H. Wright. 1981. Practical optimization. Academic press.

Thomas M. Gill, Dorothy I. Baker, Margaret Gottschalk, Peter N. Peduzzi, Heather Allore, and Amy Byers. 2002. A program to prevent functional decline in physically frail, elderly persons who live at home. *New Engl. J. Med.* 347, 14 (2002), 1068–1074.

Google. 2014. Android operating system. Retrieved from http://www.android.com.

Abdelkrim Hadjidj, Marion Souil, Abdelmadjid Bouabdallah, Yacine Challal, and Henry Owen. 2013. Wireless sensor networks for rehabilitation applications: Challenges and opportunities. *J. Netw. Comput. Appl.* 36, 1 (2013), 1–15.

David Hailey, Risto Roine, Arto Ohinmaa, and Liz Dennett. 2011. Evidence of benefit from telerehabilitation in routine care: A systematic review. *J. Telemed. Telecare* 17, 6 (2011), 281–287.

Sabrina Iarlori, Francesco Ferracuti, Andrea Giantomassi, and Sauro Longhi. 2014. RGBD camera monitoring system for Alzheimer's disease assessment using recurrent neural networks with parametric bias action recognition. In *Proceedings of the 19th World Congress the International Federation of Automatic Control (IFAC'14)*.

Carl T. Kelley. 1999. *Iterative Methods for Optimization*. Vol. 18. Siam.

Alberto Leardini, Lorenzo Chiari, Ugo Della Croce, and Aurelio Cappozzo. 2005. Human movement analysis using stereophotogrammetry: Part 3. Soft tissue artifact assessment and compensation. *Gait Posture* 21, 2 (2005), 212–225.

Sebastian O. H. Madgwick, Andrew J. L. Harrison, and Ravi Vaidyanathan. 2011. Estimation of IMU and MARG orientation using a gradient descent algorithm. In *Proceedings of IEEE International Conference on Rehabilitation Robotics*.

Robert Mahony, Tarek Hamel, and Jean-Michel Pflimlin. 2008. Nonlinear complementary filters on the special orthogonal group. *IEEE Trans. Automat. Control* 53 (2008), 1203–1218.

Mauro Marinoni, Alessandro Biondi, Pasquale Buonocunto, Gianluca Franchino, Daniel Cesarini, and Giorgio C. Buttazzo. 2017. Real-time analysis and design of a dual protocol support for bluetooth LE devices. *IEEE Trans. Industr. Informat.* 13 (2017), 80–91.

NFCForum. 2014. Bluetooth secure simple pairing using NFC. Retrieved from https://www.bluetooth.org/DocMan/handlers/DownloadDoc.ashx?doc_id=264234.

Nordic Semiconductor. 2015. *nRF52823 Product Specification v1.0*.

Alana Peters, Brook Galna, Morgan Sangeux, Meg Morris, and Richard Baker. 2010. Quantification of soft tissue artifact in lower limb human motion analysis: A systematic review. *Gait Posture* 31 (2010), 1–8.

Polhemus. 2010. *Polhemus Patriot Product Specification*.

R. Rajkumar, I. Lee, L. Sha, and J. Stankovic. 2010. Cyber-physical systems: The next computing revolution. In *Proceedings of the 47th Design Automation Conference*. DOI: http://dx.doi.org/10.1145/1837274.1837461

Trevor G. Russel. 2007. Physical rehabilitation using telemedicine. *J. Telemed. Telecare* 13 (2007), 217–220.

Thomas Seel, Jörg Raisch, and Thomas Schauer. 2014. IMU-based joint angle measurement for gait analysis. *Sensors* 14 (2014), 6891–6909.

Roland Sigrist, Georg Rauter, Robert Riener, and Peter Wolf. 2013. Augmented visual, auditory, haptic, and multimodal feedback in motor learning: A review. *Psychonom. Bull. Rev.* 20 (2013), 21–53.

Affan A. Syed and John Heidemann. 2006. Time synchronization for high latency acoustic networks. In *Proceedings of 25th IEEE International Conference on Computer Communications (INFOCOM'06)*.

Masoud Masih Tehrani. 1983. Ring laser gyro data analysis with cluster sampling technique. *Fiber Optic and Laser Sensors I*. Vol. 412. 207–221.

Xiaoping Yun and Eric R. Bachmann. 2006. Design, implementation, and experimental results of a quaternion-based kalman filter for human body motion tracking. *IEEE Trans. Robot.* 22 (2006), 1216–1227.

Zhi-Qiang Zhang, Wai-Choong Wong, and Jian-Kang Wu. 2011. Ubiquitous human upper-limb motion estimation using wearable sensors. *IEEE Trans. Info. Technol. Biomed.* 15 (2011), 513–521.

Received August 2016; revised July 2017; accepted September 2017